Published in final edited form as:
Structure. 2005 July ; 13(7): 1069–1080.

Structure of $G\alpha_{i1}$ bound to a GDP-selective peptide provides insight into guanine nucleotide exchange

Christopher A. Johnston[1], **Francis S. Willard**[1,2,3], **Mark R. Jezyk**[4], **Zoey Fredericks**[5,*], **Erik T. Bodor**[1], **Miller B. Jones**[1,2,3], **Rainer Blaesius**[5,†], **Val J. Watts**[6], **T. Kendall Harden**[1], **John Sondek**[1,2,4], **J. Kevin Ramer**[5,§], and **David P. Siderovski**[1,2,3,‡]

1 *Department of Pharmacology*

2 *Lineberger Comprehensive Cancer Center*

3 *UNC Neuroscience Center*

4 *Department of Biochemistry & Biophysics, The University of North Carolina at Chapel Hill, Chapel Hill, NC 27599-7365*

5 *Karo*Bio USA, Durham, NC 27703-8466*

6 *Department of Medicinal Chemistry and Molecular Pharmacology, School of Pharmacy, Purdue University, West Lafayette, IN 47907-2091*

* *Amgen Inc., 1201 Amgen Court West, Seattle, WA 98119*

† *Becton Dickinson, 21 Davis Drive, Research Triangle Park, NC 27709*

§ *Hemocellular Therapeutics, 5312 Farrington Road, Chapel Hill, NC 27517*

Abstract

Heterotrimeric G-proteins are molecular switches that regulate numerous signaling pathways involved in cellular physiology. This characteristic is achieved by the adoption of two principal states: an inactive, GDP-bound and an active, GTP-bound state. Under basal conditions G-proteins exist in the inactive GDP-bound state, thus nucleotide exchange is crucial to the onset of signaling. Despite our understanding of G-protein signaling pathways, the mechanism of nucleotide exchange remains elusive. We employed phage display technology to identify nucleotide-state-dependent Gα binding peptides. Herein, we report a GDP-selective Gα-binding peptide, KB-752, that enhances spontaneous nucleotide exchange of $G\alpha_i$ subunits. Structural determination of the $G\alpha_{i1}$/peptide complex reveals unique changes in the Gα switch regions predicted to enhance nucleotide exchange by creating a GDP dissociation route. Our results cast light onto a potential mechanism by which Gα subunits adopt a conformation suitable for nucleotide exchange.

Introduction

Heterotrimeric G-proteins are crucial intracellular mediators of a diverse array of extracellular signals including hormones, photons, odorants, and small molecules (Cabrera-Vera et al., 2003; McCudden et al., 2005). In the standard model of G-protein signaling, seven transmembrane domain G protein-coupled receptors (GPCRs) are associated with inactive, membrane-tethered G-protein heterotrimers consisting of Gα·GDP bound to Gβγ. Gβγ facilitates the receptor coupling of Gα·GDP, stabilizes its GDP-bound state and prevents spontaneous nucleotide exchange, thus serving as a guanine nucleotide dissociation inhibitor

‡Corresponding author: Dr. David P. Siderovski, UNC Department of Pharmacology, 1106 M.E. Jones Bldg., CB #7365, Chapel Hill, NC 27599-7365 USA tel: 1-919-843-9363; fax: 1-919-966-5640; email: dsiderov@med.unc.edu

(GDI) (Higashijima et al., 1987). Ligand-activated GPCRs serve as guanine nucleotide exchange factors (GEFs), catalyzing exchange of GDP for GTP on Gα. GTP binding alters the conformation of three flexible "switch" regions within Gα, leading to Gβγ dissociation. Both Gα·GTP and Gβγ subsequently regulate several downstream effectors including adenylyl cyclases, phospholipases, kinases, and ion channels (Cabrera-Vera et al., 2003; McCudden et al., 2005). Based on sequence similarity and functional differences in effector regulation, G proteins are grouped into four distinct families: $G\alpha_{i/o}$, $G\alpha_{s}$, $G\alpha_{q/11}$, and $G\alpha_{12/13}$ (Cabrera-Vera et al., 2003; McCudden et al., 2005). Signal termination is achieved by the intrinsic GTP hydrolysis activity of Gα and accelerated by "regulators of G-protein signaling" (RGS proteins; Neubig and Siderovski, 2002). Formation of Gα·GDP causes heterotrimer reassociation, thereby preventing further effector interactions by either Gα or Gβγ. Accordingly, the duration of G-protein signaling is determined by the lifetime of Gα in the GTP-bound state (Sprang, 1997). Thus, G-proteins serve as temporal regulators of signaling pathways and understanding the molecular determinants of their guanine nucleotide cycle is of particular interest.

Structures of Gα subunits, including $G\alpha_{i1}$, in both inactive and activated states have revealed critical conformational changes that occur during GTP binding and hydrolysis (Sprang, 1997). Gα consists of a Ras-like domain, a structural fold present in many GTPases, and a unique all-helical domain. Bound nucleotide resides in a cleft between these two domains. Although flexibility between these domains is thought to govern the rate of spontaneous nucleotide exchange (Remmers et al., 1999), the mechanism whereby Gα GEFs induce nucleotide exchange is not yet clear. Two distinct types of Gα GEFs are now known: membrane-bound GPCRs and the soluble, cytoplasmic RIC-8 proteins. The structure of the prototypical GPCR rhodopsin provided the first structural glimpse of the most prominent class of Gα GEFs (Palczewski et al., 2000); however, the receptor was in an inactive form and not bound to heterotrimer, and thus little direct information was gained about the mechanism for G-protein activation. The non-receptor Gα GEF RIC-8 is widely conserved across metazoa as a critical determinant (along with $G\alpha_{i}$ subunits) in mitotic spindle force generation during mitosis (reviewed in McCudden et al., 2005). Unlike the GEFs for Ras-superfamily GTPases, such as the RhoGEF family (Rossman et al., 2005), that have no preference for nucleotide state (GDP- or GTP-bound), RIC-8 exhibits selective interaction with the GDP-bound state of Gα subunits and does not bind nor act as a GEF toward Gα·GTP (Afshar et al., 2004; Tall et al., 2003). As RIC-8 proteins have only been recently discovered, structural studies of these proteins have yet to be reported. Thus, the structural determinants of Gα activation by GEFs remain largely unknown.

Phage display is a powerful technique to identify small peptides capable of binding desired targets in an unbiased manner. Identified peptides can then serve as tools to study target protein binding surfaces, protein-protein interaction sites, and protein function and regulation (reviewed in Rodi et al., 2002). This technology has identified peptide modulators of a variety of enzyme classes and signaling molecules (*e.g.*, Ashraf et al., 2003; Hyde-DeRuyscher et al., 2000). In particular, phage display and similar approaches have been used to investigate G-protein binding interfaces on GPCRs (Gilchrist et al., 1998; Martin et al., 1996) and effector binding regions on Gβγ subunits (Scott et al., 2001), as well as to identify peptides with G-protein regulatory properties, including both GEF and GDI activities (Hessling et al., 2003; Ja and Roberts, 2004). In the present study, we have identified guanine nucleotide-dependent Gα binding peptides from a phage display peptide library. In particular, we describe the guanine nucleotide exchange factor activity of a GDP-selective peptide, termed KB-752. To understand the mechanism of KB-752 GEF activity, we determined the crystal structure of the peptide bound to $G\alpha_{i1}$. These studies are the first to describe the structure of a Gα subunit in complex with a GEF and provide direct structural evidence in support of a previously proposed mechanism for the GPCR-catalyzed nucleotide exchange reaction.

Results

Identification of nucleotide-dependent Gα binding peptides

We used phage display to obtain peptides that recognize the distinct conformations of Gα when bound to GDP *versus* GTPγS (Cabrera-Vera et al., 2003; Sprang, 1997). Biotinylated $G\alpha_{i1}$·GDP and $G\alpha_{i1}$·GTPγS were independently immobilized onto streptavidin-coated microtiter plates for selection of phage-displayed peptides. Phage selectivity was monitored by comparing phage ELISA signals between wells containing $G\alpha_{i1}$ and wells blocked with albumin. After four iterative rounds of selection, clonal bacteriophage isolates were purified, amplified and screened for selective binding to $G\alpha_{i1}$ in GDP- or GTPγS-bound states (*e.g.*, Figure 1A). In total, we isolated 51 GDP-dependent, 12 GTPγS-dependent, and 5 nucleotide-state-independent phage-displayed peptides. Extensive database searches suggest that none of these peptides has sequence similarity to known Gα interacting proteins (data not shown).

A representative group of GDP-dependent phage (Figure 1B) showed strong sequence similarity around the motif $TWX^{E}/_{D}FL$. Of these GDP-selective peptides, we focused initially on KB-752. Nucleotide-dependent Gα binding was quantitated by surface plasmon resonance (SPR) measurements on a streptavidin biosensor chip coated with biotinylated KB-752 (*e.g.*, Figure 1C for $G\alpha_{i1}$). Dissociation constants (K_d values) were obtained by simultaneous kinetic analysis of on (k_a) and off (k_d) rates obtained by injecting increasing concentrations of Gα in GDP-, GDP·AlF_4^-, and GTPγS-bound states (*e.g.*, Figure 1D for $G\alpha_{i1}$·GDP). In agreement with the phage selection, KB-752 displayed highest affinity binding to $G\alpha_{i1}$ in its GDP-bound form (K_d of 3.9 ± 0.6 μM). No appreciable binding was observed to the transition-state-mimetic form of $G\alpha_{i1}$·GDP·AlF_4^-, although measurable (albeit low affinity) binding was observed for $G\alpha_{i1}$·GTPγS (K_d of 28.0 ± 3.2 μM); given the slow rate of spontaneous nucleotide exchange of $G\alpha_{i1}$ (Fields and Casey, 1997), this observed binding may be due to residual GDP-bound protein. KB-752 demonstrated lower affinity for the closely-related $G\alpha_o$, with a K_d of 18.2 ± 3.0 μM for $G\alpha_o$·GDP, but no measurable interaction to GDP·AlF_4^- nor GTPγS-bound forms of $G\alpha_o$ (data not shown).

KB-752 binding affects guanine nucleotide exchange

To examine the effects of KB-752 on nucleotide exchange by Gα binding partners, [^{35}S] GTPγS binding to purified Gα was quantified in the absence or presence of peptide. KB-752 enhanced the nucleotide exchange rate of $G\alpha_{i1}$ (Figure 2A); the effective concentration for 50% maximal response (EC_{50}) for KB-752 GEF activity on $G\alpha_{i1}$ was 5.6 ± 1.1 μM (Figure 2B), comparable to its observed K_d. Equipotent GEF activity was found for both $G\alpha_{i2}$ and $G\alpha_{i3}$ (Figure 2B). KB-752 did not affect the nucleotide exchange rate of $G\alpha_{i2}\beta_1\gamma_2$ (Figure 2C), suggesting that KB-752 cannot disrupt a native heterotrimer and interacts solely with free Gα.

Despite binding to $G\alpha_o$·GDP, KB-752 did not affect nucleotide exchange even at saturating concentrations (Figure 2D). We hypothesized that the higher intrinsic rate of spontaneous nucleotide exchange of $G\alpha_o$ *vs* $G\alpha_i$ contributes to the lack of KB-752 activity on $G\alpha_o$. To test this, we purified $G\alpha_{i1}$ containing an arginine-144 to alanine (R144A) mutation that disrupts an interaction between the all-helical and Ras-like domains, and thus renders the spontaneous exchange rate equivalent to that of $G\alpha_o$ (Remmers et al., 1999); confirmed in Figure 3A). KB-752 did not enhance the exchange rate of $G\alpha_{i1}$ (R144A) (Figure 3B), highlighting the mechanism of KB-752 as enhancing GDP release from the intrinsically slow exchanger $G\alpha_i$.

To validate these results, we employed steady-state GTPase assays. Given that GDP release is the rate-limiting step of the Gα guanine nucleotide cycle, any alteration of GDP release, either positively (*i.e.*, GEF activity) or negatively (*i.e.*, GDI activity), will be reflected in the overall steady-state rate of GTP hydrolysis (Ross, 2002). KB-752 enhanced steady-state GTP

hydrolysis by $G\alpha_{i1}$ (Figure 3C), further indicating that it has GEF activity for $G\alpha_i$ subunits. No effect of KB-752 was seen on $G\alpha_o$. These results support the conclusion that KB-752 possesses $G\alpha_i$-selective GEF activity.

Structure of KB-752 bound to α_{i1}

To ascertain the molecular mechanism of KB-752 GEF activity, we determined the structure of KB-752-bound $G\alpha_{i1}$·GDP (PDB ID 1Y3A; Figure 4 and Table 1). KB-752 assumes a partial α-helical structure and binds $G\alpha_{i1}$ between switch II and the α3 helix of the Ras-like domain (Figures 4 and 5A). The repositioning of switch II affords the binding groove for KB-752, as the α3 helix is not significantly altered in conformation compared to other structures of $G\alpha_{i1}$. Indeed, the ability to reposition switch II likely defines the nucleotide specificity of KB-752 binding, given predicted steric hindrance between the N-terminus of KB-752 and switch II within $G\alpha_{i1}$·GTPγS and $G\alpha_{i1}$·GDP·AlF_4^- (Figure 5B). In particular, the positioning of tryptophan-211 of switch II would not accommodate tryptophan-5 of KB-752 (Figure 5B); however, tryptophan-211 is repositioned in the $G\alpha_{i1}$·GDP/KB-752 structure and creates part of a critical hydrophobic pocket used by KB-752 for binding (see below).

The switch II/α3 helix binding pocket for KB-752 is similar to that of the N-terminal alpha-helix of the RGS14 GoLoco motif, a short polypeptide that displays GDI activity toward $G\alpha_{i1}$ (PDB ID 1KJY) (Kimple et al., 2002); however, the GoLoco motif binding site extends into the all-helical domain (Figure 5C), whereas KB-752 makes no contacts with this region of $G\alpha_{i1}$ (Figure 5A). The lack of functional contacts made between KB-752 and the all-helical domain was validated using a chimera ("Gαioi") with the Ras-like domain of $G\alpha_{i1}$ but the all-helical domain of $G\alpha_o$ (Remmers et al., 1999); KB-752 displays GEF activity on this chimera equal to that on wildtype $G\alpha_{i1}$ (Figure 5D), suggesting that interactions with the Ras-like domain are sufficient for GEF activity. The use of a switch II/α3 helix binding pocket for both KB-752 and GoLoco motif peptides was also validated biochemically. The GEF activity of KB-752 on $G\alpha_{i1}$ was found to be competitively antagonized by the GoLoco motif of the RGS14 paralogue, RGS12 (Figure 5E). Unlike the GoLoco motif, which lies over the GDP-binding pocket and uses an arginine finger to stabilize GDP (Kimple et al., 2002), KB-752 does not occlude nor make contact with GDP (Figure 5A vs 5C), suggesting that its GEF activity relies on conformational changes induced within $G\alpha_{i1}$. In support of these distinct modes of interaction about the GDP-binding pocket, KB-752 binding has almost no effect on the rate by which $G\alpha_{i1}$ is activated by aluminum tetrafluoride (Fig. 5F), unlike the inhibitory effect of GoLoco motif peptides (Willard et al., 2004).

Structural basis for the conserved $TWX^E/_DFL$ binding motif

Figure 6 shows specific contacts between KB-752 and $G\alpha_{i1}$. Glutamate-11 (E11) of KB-752 forms a salt bridge with R208 of $G\alpha_{i1}$. Tryptophan-5 (W5) is found within a hydrophobic pocket formed by F215, L249, and I253 of $G\alpha_{i1}$. Phenylalanine-8 (F8) is also placed within a hydrophobic environment established by W211, I212, and F215 of $G\alpha_{i1}$. The burial of large hydrophobic residues within the hydrophobic groove between switch II and the α3 helix is common among several known Gα binding partners: p115RhoGEF-RGS inserts a methionine (M165) into the $G\alpha_{i/13}$ chimera (Chen et al., 2005), the C2 domain of adenylyl cyclase inserts a phenylalanine (F991) into $G\alpha_s$ (Tesmer et al., 1997b), and the gamma subunit of cGMPphosphodiesterase inserts a tryptophan (W70) into $G\alpha_t$ (Slep et al., 2001). Burial of the peptide residues W5 and F8 within $G\alpha_{i1}$ validates the results of the phage selection, as these two hydrophobic residues figure prominently within the $TWX^E/_DFL$ binding motif (Figure 1B). An intramolecular hydrogen bond network between threonine-4 (T4) and both the side-chain carboxylate and peptide-bond nitrogen of aspartate-7 (D7) (Figure 6B) underscores the conservation of threonine and acidic residues within the $TWX^E/_DFL$ motif. Specifically, the side-chain hydroxyl of T4 forms a hydrogen bond with both the side-chain carboxylate and

main-chain amide nitrogen of D7, and the main-chain carbonyl oxygen of T4 forms a hydrogen bond with the main-chain amide nitrogen of D7. Additionally, this hydrogen bonding network within the α-helical portion of KB-752 serve to orient both W5 and F8 side chains toward the α binding face of the peptide.

Based on contacts between KB-752 and $G\alpha_{i1}$, we generated three KB-752 variants to validate biochemically the structural model. E11 was replaced with leucine to eliminate the ionic interaction with R208. W5 and F8 of the $TWX^{E}/_{D}FL$ motif were each independently replaced with alanine to reduce the potential for burial within hydrophobic environments created by switch II and the α3 helix. We first confirmed by SPR that each mutation abrogated $G\alpha_{i1}$ binding. $G\alpha_{i1}$·GDP was capable of interacting with the E11L peptide, but binding was significantly attenuated compared to wild-type (Figure 6C). Both W5A and F8A peptides displayed a near complete loss of binding to $G\alpha_{i1}$·GDP. We then tested the ability of each peptide to enhance nucleotide exchange by $G\alpha_{i1}$·GDP. Wild-type KB-752 resulted in an approximately 3-fold increase in the rate of [^{35}S]GTPγS binding. The E11L peptide had diminished GEF activity compared to wild-type (Figure 6D), while W5A and F8A peptides lacked significant GEF activity. These results corroborate the critical contacts made between $G\alpha_{i1}$ and these residues of KB-752 in the structural model.

Structural basis for KB-752 GEF activity

Exchange of GDP for GTP results in movement of the three switch regions to stabilize bound GTP and adopt the conformation responsible for effector binding (Sprang, 1997). $G\alpha_{i1}$·GDP/KB-752 possesses significant alterations in each switch region compared to $G\alpha$·GDP/$G\beta_1\gamma_2$ (Figure 7A). Most apparent is switch II, which is displaced down and outward compared to the $G\alpha_{i1}$·GDP/$G\beta_1\gamma_2$ structure (Wall et al., 1995). This movement results in the lip of switch II, normally ordered and helical in the GTPγS-bound state (Coleman et al., 1994; Sunahara et al., 1997), being displaced away from the nucleotide binding pocket and GDP. This conformation in $G\alpha_{i1}$·GDP/KB-752 contrasts with the movement of switch II *towards* the nucleotide pocket when GTPγS is bound. Switch III is also slightly displaced from GDP within KB-752-bound $G\alpha_{i1}$ compared to the heterotrimer (Figure 7A). However, of the four $G\alpha_{i1}$/KB-752 dimers in the asymmetric unit (Table 1), only one $G\alpha_{i1}$ molecule (chain B of PDB ID 1Y3A) had sufficient electron density to accurately model the switch III loop, suggesting that this region of $G\alpha_{i1}$ is inherently flexible even when bound to KB-752. Similar alterations to both switch regions II and III are seen in GoLoco-bound $G\alpha_{i1}$ ($G\alpha_{i1}$·GDP/R14GL) (Kimple et al., 2002); however, switch II is more dramatically displaced in $G\alpha_{i1}$·GDP/KB-752 (Figure 7B). Interestingly, despite movement in switch II, the β3/α2 loop at the entry to switch II is not significantly displaced in the $G\alpha_{i1}$·GDP/R14GL structure compared to the $G\alpha_{i1}$·GDP/$G\beta_1\gamma_2$ structure (Figure 7A vs. B). In contrast, this β3/α2 loop is removed from the guanine nucleotide pocket along with switch II in the $G\alpha_{i1}$·GDP/KB-752 structure (Figure 7B). Displacement of the β3α2 loop is stabilized through several interactions with KB-752, including hydrogen bonding between the carbonyl oxygen of glycine-202 of the β3/α2 loop and the indole nitrogen of tryptophan-5 in KB-752 (Figure 7C), indicating an additional role for this key peptide residue. The displacement of switch II positions the catalytic glutamine-204 residue far from the nucleotide binding pocket compared to structures of $G\alpha_{i1}$·GTPγS and $G\alpha_{i1}$·GDP·AlF_4^- (Figure 8), and this residue makes an intramolecular bond with valine-201 (Figure 7C).

Switch I within $G\alpha_{i1}$·GDP/KB-752 adopts a conformation more similar to the activated states of $G\alpha_{i1}$·GTPγS and $G\alpha_{i1}$·GDP·AlF_4^- (Figure 8), moving in closer proximity to GDP (compared to Gβγ- and GoLoco-bound states) and affecting the position of arginine-178 (R178) (Figure 8A). In the $G\alpha_{i1}$·GDP/$G\beta_1\gamma_2$ heterotrimer (PDB 1GP2) (Wall et al., 1995), R178 of switch I forms a salt-bridge interaction with glutamate-43 (E43) across the bound GDP (Figure 8A).

This "seatbelt" conformation, resulting from reoriented coordinating residues N149 and D150 due to $G\beta_1\gamma_2$ binding (Wall et al., 1998), is proposed to stabilize bound GDP (Lambright et al., 1996;Wall et al., 1995). This same interaction occurs in $G\alpha_{i1}$·GDP/R14GL (Kimple et al., 2002) (Figure 8A), but not in the structures of free $G\alpha_{i1}$·GDP (Wall et al., 1998) suggesting that the formation of this R178/E43 salt-bridge represents a common mechanism used by GDIs for $G\alpha_{i1}$. Interestingly, in the KB-752-bound structure, the seatbelt interaction is not present (Figure 8A, B); the conformation of R178 is nearly identical to that of the $G\alpha_{i1}$·GDP·AlF_4^- transition state (PDB 1GFI) (Figure 8C) (Coleman et al., 1994) in which R178 is oriented to participate in GTP hydrolysis by stabilization of the leaving γ-phosphate group as mimicked by the aluminum tetrafluoride anion. These findings suggest that the R178/E43 interaction is broken during nucleotide exchange and that an "unbuckled seatbeat" conformation may be essential for GDP release in addition to GTP hydrolysis. Thus, KB-752 appears to alter switch I and II to create a feasible exit route for GDP (see Discussion below). Magnesium was not observed in the nucleotide binding pocket of $G\alpha_{i1}$·GDP/KB-752 (although its coordinating residue T181 is unaltered; Figure 8C,D), consistent with studies showing that Mg^{2+} has no effect on GDP binding to Gα (*e.g.*,Higashijima et al., 1987).

Discussion

Despite many biochemical and structural studies of the guanine nucleotide cycle, the mechanism of heterotrimeric G-protein activation remains elusive. Mutagenesis studies have highlighted several determinants governing the G-protein coupling and nucleotide exchange properties of GPCRs (Bourne, 1997; Hamm, 2001), but precisely how a Gα subunit is induced to exchange GDP for GTP has remained unanswered, given the inherent difficulty in obtaining structural information on the GPCR:G-protein complex. Structural determinants of the recently described GEF activity of RIC-8 (Afshar et al., 2004; Tall et al., 2003) are also not known.

An alternative approach has been the use of small peptides that possess nucleotide-dependent binding and biochemical properties akin to known G-protein regulators. Mastoparan, a 14 aa peptide found in wasp venom, is a GEF for $G\alpha_i$ and $G\alpha_o$ (Higashijima et al., 1990). The solution structure of mastoparan bound to $G\alpha_i$ indicates a helical conformation for this peptide; however, biochemical studies suggest its binding interface resides at the extended N-terminus of Gα (Sukumar and Higashijima, 1992). Moreover, mastoparan (INLKALAALAKKIL) shows no similarity to the $TWX^E/_DFL$ motif found in KB-752 and other Gα·GDP binding peptides from our screen. Synthetic peptides from the third intracellular loop of several GPCRs, a region involved in G-protein coupling and activation by receptor, have also been used to study G protein activation. A solution structure of a peptide from the third intracellular loop of the CB1 cannabinoid receptor suggests the necessity for a helical conformation (Ulfers et al., 2002). Finally, phage display has identified short hepta-peptides with biochemical activity at specific G-protein subunits (Hessling et al., 2003), although no structural information has been reported. Our results further highlight the power of phage display as a useful technique to identify conformation-dependent binding peptides that can be useful tools to investigate protein function. The structure of the $G\alpha_{i1}$·GDP/KB-752 complex clearly demonstrates the basis of nucleotide specificity of this peptide.

Furthermore, our structural determination of KB-752 bound to $G\alpha_{i1}$ represents the first glimpse of a Gα subunit bound to a GEF. As with other Gα regulators, KB-752 modulates the conformation of the switch regions critical to the guanine nucleotide cycle (Sprang, 1997). Previous structures of uncomplexed $G\alpha_{i1}$·GDP have revealed structural disorder in these switch regions, particularly switch II and III (Coleman and Sprang, 1998). However, structures in which $G\alpha_{i1}$ is bound to regulators (Gβγ, RGS4, GoLoco motif) or in the activated state (GTPγS- or GDP·AlF_4^--bound), the switch regions become ordered in specific, defined conformations (Coleman et al., 1994; Kimple et al., 2002; Tesmer et al., 1997a; Wall et al.,

1995). Similarly, our structure of $G\alpha_{i1}$·GDP/KB-752 reveals order in the switch regions, suggesting that the peptide stabilizes this conformation resulting in its GEF activity -- specifically by creating a stabilized route for GDP egress.

Since the Gα nucleotide binding pocket is buried far from the proposed Gα/receptor interacting surface, it is thought that GPCRs use Gβγ as a lever to “pull open” Gα, creating a GDP exit route. By modeling onto Gα the structural changes in EF-Tu induced by EF-Ts during nucleotide exchange, Bourne and colleagues have pointed to the β3/α2 loop as a potential "lip" that occludes GDP release (Iiri et al., 1998). Gβγ makes several contacts with this region and has been proposed to use additional contacts within the α2 helix (switch II), namely D228 of $G\beta_1$ contacting K210 in $G\alpha_{i1}$ (K206 in $G\alpha_s$), to lever open the lip to induce GDP release (Rondard et al., 2001). GPCRs are thought to use the Gα N-terminus to tilt Gβγ (making extensive contacts with the Gα N-terminus) away from Gα, thereby opening the β3/α2 lip (Iiri et al., 1998). Our structure of the GEF peptide KB-752 bound to $G\alpha_{i1}$ supports the Bourne model. By binding between the switch II and α3 helices, KB-752 pushes the α2 helix away from nucleotide, similar to the proposed levering action of Gβγ. Displacement of switch II results in the β3/α2 loop (part of the proposed occlusive lip (Iiri et al., 1998)) also being pulled away from nucleotide in a way that might allow more efficient GDP egress. Whereas switch II is displaced by the binding of the RGS14 GoLoco peptide, the β3/α2 loop remains essentially unaltered in conformation compared to the Gβγ-bound, heterotrimeric structure. These results further highlight the potential role of the β3/α2 loop as an occlusive lip preventing GDP release, as both Gβγ and GoLoco (each with GDI activity) position the β3/α2 loop to block the proposed GDP egress route, whereas KB-752 (with GEF activity) removes the loop from this position. Importantly, not only does KB-752 displace the β3/α2 loop from its occlusive orientation but also makes several contacts with this loop, which presumably serves to stabilize its reorientation. Although the precise structural determinants of GPCR-mediated GEF activity will clearly be distinct from that of our artificial phage-display peptide GEF, the structural changes in $G\alpha_{i1}$ induced by KB-752 provide support for the Gβγ-levering model of receptor GEF function by suggesting that repositioning of switch II and the β3/α2 loop is critical for GDP release. In this model, the proposed egress route for GDP is towards the Gβγ binding face of Gα, which is more accessible following the displacement of the occlusive β3/α2 loop.

An alternative opinion on receptor-mediated heterotrimer activation (Cherfils and Chabre, 2003) suggests that GPCRs use the Gα N-terminus to maneuver Gβγ in an opposite fashion to that proposed in the Bourne model. In this “gear-shift” model, Gβγ is shifted *towards* Gα resulting in a closely packing Gα-Gβ interface stabilized by a proposed binding of the Gγ N-terminus to the Gα helical domain (Cherfils and Chabre, 2003). This Gβγ shift is proposed to alter the conformation of the α5 helix, previously implicated in the receptor-catalyzed nucleotide exchange reaction (Marin et al., 2002). Our structure of $G\alpha_{i1}$·GDP/KB-752, while not invalidating the receptor GEF model of Cherfils and Chabre given lack of sequence similarity between KB-752 and known Gα regulators, certainly does not support their model of GPCR GEF activity for three reasons: (*i*) KB-752 causes switch II to be displaced away from the GDP pocket rather than being packed more tightly, (*ii*) the proposed GDP exit route induced by KB-752 binding is on the Gβ-binding face, and (*iii*) KB-752 does not cause significant alterations in α5 helix conformation.

In addition to affecting switch II (α2 helix) and maneuvering the β3/α2 loop in a manner consistent with the Gβγ-lever model (Iiri et al., 1998), KB-752 binding also alters switch I. In contrast to displacement of switch II *away* from the nucleotide binding pocket, switch I is displaced slightly *towards* this pocket into a similar conformation to that of GTPγS- and GDP·AlF_4^--bound Gα. In the $G\alpha_{i1}$·GDP/$G\beta_1\gamma_2$ heterotrimer and $G\alpha_{i1}$·GDP/R14GL complex, R178 of switch I forms a salt bridge with E43 (an interaction not observed in free $G\alpha_{i1}$·GDP), forming a “seatbelt” over bound GDP thought to aid in the stabilization of Gα·GDP by Gβγ or

GoLoco binding (Kimple et al., 2002; Lambright et al., 1996; Wall et al., 1995). Switch I in the $G\alpha_{i1}$·GDP/KB-752 structure reveals an R178 conformation out of bonding distance to E43, similar to that seen in the structure of free $G\alpha_{i1}$·GDP, in which R178 is thought to be quite flexible (Mixon et al., 1995). The loss of the R178/E43 interaction in both the $G\alpha_{i1}$·GDP/KB-752 (GEF) structure as well as free $G\alpha_{i1}$·GDP (which has higher spontaneous nucleotide exchange compared to Gβγ-bound) supports the loss of this interaction as coinciding with nucleotide exchange. Thus, breaking the R178/E43 "GDP seatbelt" is a potentially crucial step in GDP release and subsequent GTP binding. Surprisingly, the R178 side chain is in a nearly identical conformation in the $G\alpha_{i1}$·GDP/KB-752 structure compared to the $G\alpha_{i1}$·GDP·AlF_4^- structure (Figure 7B), indicating that this residue potentially adopts a conformation that is suitable for both GDP/GTP exchange and GTP hydrolysis. Having the R178/E43 interaction disrupted, along with creating a feasible exit route by modulating the switch II helix, may contribute to enhanced GDP release and, thus, an enhanced nucleotide exchange rate observed upon KB-752 binding.

Despite the GEF activity of KB-752 *towards* $G\alpha_{i1}$, the structure of the complex contains bound GDP. This seemingly paradoxical observation is explained by several considerations. The nucleotide-free state of isolated Gα is very unstable, likely reflecting an instantaneous conformation as nucleotide binding is extremely rapid (Ferguson et al., 1986; Sprang, 1997); stable trapping of the nucleotide-free state has only recently been successfully described following binding to the non-receptor GEF RIC-8 (Tall and Gilman, 2004). The Gα/RIC-8 interface is likely more extensive than with the small KB-752 peptide, which would add substantial stability to the nucleotide-free conformation. Similarly, establishing the nucleotide-free state of small GTPases also necessitates a large stabilizing interface with respective GEFs (*e.g.*, Worthylake et al., 2000) that cannot be provided by the small KB-752 peptide. Along with the fact that the $G\alpha_{i1}$ /KB-752 complex was crystallized in the presence of 5 μM GDP, these factors likely impeded the chances of capturing $G\alpha_{i1}$ in a nucleotide-free state.

In conclusion, our identification and structural analysis of a novel Gα·GDP binding peptide with GEF activity towards $G\alpha_{i1-3}$ subunits provides support of the "Gβγ lever" hypothesis of GPCR GEF activity. The activity of KB-752 as a GEF for $G\alpha_i$ suggests a future utility of this peptide as a new molecular tool to study heterotrimeric G-protein signaling *in vitro* and *in vivo*.

Experimental Procedures

Unless otherwise noted, all reagents were from Sigma. Peptides were synthesized by Anaspec (San Jose, CA). Biotinylated peptides were synthesized by Dr. Michael Berne and colleagues of the Tufts University Core Facility: biotinylation was performed on resin-bound, Fmoc group-protected synthetic peptides that were selectively deprotected only at their N-termini, assuring biotin conjugation solely at the free amine.

Phage selection. Biotinylated $G\alpha_{i1}$ was purified from *E. coli* as described (Kimple et al., 2004): presence of an N-terminal AviTag sequence (GLNDIFEAQKIEWHE) allowed for selective *in vivo* biotinylation on the lysine residue during expression in *E. coli* strain AVB 100 that also expresses biotin ligase (BirA) and fermentation in free biotin-containing medium as per manufacturer's instructions (Avidity LCC, Denver, CO). Nineteen different, random peptide bacteriophage libraries were obtained from New England Biolabs (PhD7, PhD12) or prepared by Karo*Bio USA using published methods (Sparks et al., 1996). Immulon 4 plates (96-well; Dynatech) were coated with streptavidin in 0.1 μ$NaHCO_3$, blocked with 1.0% BSA in 0.1 M $NaHCO_3$, then incubated for 1 hr at 25 °C with 10 pmoles/well of biotin-$G\alpha_{i1}$ in buffer A (20 mM HEPES pH 7.5, 1 mM EDTA, 16 mM $MgCl_2$, 1 mM DTT, 0.05% Tween-20) with either 5 μM GDP or GTPγS. Iterative selection of binding phage was performed using

published methods (Sparks et al., 1996). Briefly, after incubating phage libraries with immobilized biotin-$G\alpha_{i1}$ for 3 hrs at 25 °C, non-specifically bound phage were removed by washing with TBST buffer (10 mM Tris-HCl pH 8.0, 150 mM NaCl, 0.05% Tween-20) with 0.5 mM biotin. Bound phage were eluted sequentially with a low pH glycine buffer and a high pH ethanolamine buffer; after neutralizing the pH, phage were amplified and subjected to repeat rounds of selection (Sparks et al., 1996).

After 4 iterations, clonal phage isolates were purified, amplified, and sequenced as described (Sparks et al., 1996). To detect bound phage by ELISA, biotin-$G\alpha_{i1}$ was incubated overnight in buffer A with either 100 μM GDP or GTPγS and then 1 pmol $G\alpha_{i1}$/well (or buffer A alone) was immobilized onto plates as previously described. 5 μL phage was added to each well in buffer A with either 100 μM GDP or GTPγS and incubated for 30 min. at 25 °C. Unbound phage was removed by TBST washes and bound phage detected with an anti-M13 antibody/horseradish peroxidase conjuguate. Assays were developed for 10 min at room temperature by adding 2,2-azinobis(3-ethylbenzothiazoline)-6 sulfonic acid and H_2O_2. Signal development was stopped by adding SDS to a final concentration of 1%.

Protein purification. His_6-tagged human $G\alpha_{i1}$ (full length, R144A mutant, and N-end 25 aa truncated) and human $G\alpha_{oA}$ (full length) were purified from BL21(DE3) *E. coli* as previously described (Kimple et al., 2004). $G\alpha_{i1}$ and $G\alpha_o$ were induced at an OD_{600} = 0.8 with 1 mM IPTG for 4 hr at 37 °C. $G\alpha_{i2}\beta_1\gamma_2$ was purified from Sf9 insect cells co-infected with baculoviruses encoding $G\alpha_{i2}$,$G\beta_1$, and His_6-Gγ2 as previously described (Hooks et al., 2003). Proteins were purified by Ni^{2+}-NTA, anion exchange, and size exclusion chromatographies as described (Hooks et al., 2003; Kimple et al., 2004). All proteins were concentrated using YM-10 centrifugal filters (Millipore).

Surface plasmon resonance (SPR) biosensor measurements. SPR binding assays were performed at 25 °C on a BIAcore 3000. To analyze nucleotide-dependent Gα binding, N-terminally biotinylated KB-752 (diluted to 0.1 μg/ml in BIA running buffer [10 mM HEPES, pH 7.4, 150 mM NaCl, 10 mM $MgCl_2$, 0.005 % NP40]) was coupled to separate flow cells of streptavidin biosensors (Biacore) using MANUAL INJECT to a surface density of ~250, ~500, or ~1000 resonance units. Prior to injection, Gα subunits were diluted in BIA running buffer with 100 μM GDP, 100 μM GDP plus 30 μM $AlCl_3$ and 10 mM NaF, or 100 μM GTPγS and incubated at 25 °C for 2-3 hr. 30 μl Gα subunit was then simultaneously injected (using KINJECT) over flow cells at 10 μl/min followed by 300 s dissociation. Binding to a non-Gα interacting, biotinylated peptide (mNOTCH1; ref. Snow et al., 2002) was subtracted from all binding curves to correct for nonspecific binding and buffer shifts. Surfaces were regenerated with two 10 μl pulses of 500 mM NaCl / 25 mM NaOH at 20 μl/min. Binding curves and kinetic analyses were conducted using BIAevaluation ver. 3.0 and plotted using GraphPad Prism ver. 4.0b. Binding affinities were calculated using the simultaneous association (k_a) and dissociation (k_d) analysis parameter using generated sensorgram curves.

Gα nucleotide cycle assays. GTPγS exchange assays were conducted using a nitrocellulose filter binding method (Afshar et al., 2004), with GTPγS binding reactions performed at either 20 °C ($G\alpha_o$ and $G\alpha_{i1}$-R144A) or 30 °C ($G\alpha_{i1, i2, i3}$ and $G\alpha_{i2}\beta_1\gamma_2$). Steady-state GTPase assays were carried out using a charcoal precipitation-based method (Afshar et al., 2004), with reactions incubated at 20 °C ($G\alpha_o$) or 30 °C ($G\alpha_i$) for 30 min.

Crystallization and structure determination. Crystals of KB-752 bound to $G\alpha_{i1}$ were obtained by vapour diffusion from hanging drops (3 μL) containing a 1:1 (v/v) ratio of protein solution (6 mg/ml $G\alpha_{i1}\Delta N25$ and 1.3-fold molar excess KB-752 in 20 mM Tris, pH 7.5, 20 mM NaCl, 1 mM $MgCl_2$, 10 μM GDP, 1 mM DTT, 5 % glycerol) to well solution (50 mM sodium citrate, pH 5.0, 10 % (w/w) PEG-8000, 10 % (w/w) sucrose). Crystals formed in 3-5

days at 4 °C in the space group $P2_1$ (a = 72.9 Å, b = 112.8 Å, c = 109.5 Å, α = 90°, β = 93.7°,γ= 90°), with four $G\alpha_{i1}$·GDP/KB-752 heterodimers in the asymmetric unit. To collect data at 100K, crystals were cryoprotected in 30% glycerol for 1 min then submerged in liquid N_2. A native data set was collected at the SER-CAT 22-ID beamline at APS, Argonne National Laboratory. Data was scaled and indexed using the program HKL2000. The structure of $G\alpha_{i1}$·GDP·Mg^{2+} (PDB accession code 1BOF), excluding the 25 aa N-terminus, aa 177-184 (switch I), aa 200-218 (switch II) and aa 233-239 (switch III), and waters and sulphates, was used for molecular replacement with AMoRe (Navaza, 1994). Model building was done in$_o$ (Jones et al., 1991) with successive rounds of simulated annealing, minimization, B group, and torsion angle refinements being completed using CNS (Brunger et al., 1998). All refinement was completed with non-crystallographic symmetry restraints and each of the 4 $G\alpha_{i1}$·GDP/KB-752 dimers are essentially identical. Electron density maps for model building as well as the simulated annealing composite omit map were generated using CNS. $G\alpha_{i1}$ residues 26-33 (extreme N-terminus), 113-116 (αB-αC loop, dubbed 'switch IV', within the all-helical domain; Mixon et al., 1995), and 345-354 (extreme C-terminus) were not included in the final model given incomplete electron density; prior to removal, each region had refined B-factors of >150 indicative of low statistical certainty and relative disorder. Additionally, in 3 of the 4 $G\alpha_{i1}$ subunits (molecules 'A', 'C', and 'D') in the asymmetric unit, residues 234-239 of switch III were removed from the final model. All structural images were made using PyMol (DeLano Scientific, San Carlos, CA, USA).

Acknowledgements

We thank Dr. Richard Neubig for Gαioi and Drs. Dana Fowlkes and Elliott Ross for early guidance on this project. F.S.W. and M.B.J. are postdoctoral fellowthe American Heart Association and the PhRMA Foundation, respectively. This work was supported in part by Karo*Bio USA and by NIH grants R01 GM062338 (to D.P.S.), and P01 GM065533 (to T.K.H., J.S., and D.P.S.). Use of the Advanced Photon Source was supported by the U.S. Department of Energy, Office of Basic Energy Sciences, under Contract No. W-31-109-Eng-38.

References

Afshar K, Willard FS, Colombo K, Johnston CA, McCudden CR, Siderovski DP, Gonczy P. RIC-8 is required for GPR-1/2-dependent Galpha function during asymmetric division of C. elegans embryos. Cell 2004;119:219–230. [PubMed: 15479639]

Ashraf SS, Anderson E, Duke K, Hamilton PT, Fredericks Z. Identification and characterization of peptide probes directed against PKCalpha conformations. J Pept Res 2003;61:263–273. [PubMed: 12662360]

Bourne HR. How receptors talk to trimeric G proteins. Curr Opin Cell Biol 1997;9:134–142. [PubMed: 9069253]

Brunger AT, Adams PD, Clore GM, DeLano WL, Gros P, Grosse-Kunstleve RW, Jiang JS, Kuszewski J, Nilges M, Pannu NS, et al. Crystallography & NMR system: A new software suite for macromolecular structure determination. Acta Crystallogr D Biol Crystallogr 1998;54:905–921. [PubMed: 9757107]

Cabrera-Vera TM, Vanhauwe J, Thomas TO, Medkova M, Preininger A, Mazzoni MR, Hamm HE. Insights into G protein structure, function, and regulation. Endocr Rev 2003;24:765–781. [PubMed: 14671004]

Chen Z, Singer WD, Sternweis PC, Sprang SR. Structure of the p115RhoGEF rgRGS domain-Galpha13/i1 chimera complex suggests convergent evolution of a GTPase activator. Nat Struct Mol Biol 2005;12:191–197. [PubMed: 15665872]

Cherfils J, Chabre M. Activation of G-protein Galpha subunits by receptors through Galpha-Gbeta and Galpha-Ggamma interactions. Trends Biochem Sci 2003;28:13–17. [PubMed: 12517447]

Coleman DE, Berghuis AM, Lee E, Linder ME, Gilman AG, Sprang SR. Structures of active conformations of Gi alpha 1 and the mechanism of GTP hydrolysis. Science 1994;265:1405–1412. [PubMed: 8073283]

Coleman DE, Sprang SR. Crystal structures of the G protein Gi alpha 1 complexed with GDP and Mg2+: a crystallographic titration experiment. Biochemistry 1998;37:14376–14385. [PubMed: 9772163]

Ferguson KM, Higashijima T, Smigel MD, Gilman AG. The influence of bound GDP on the kinetics of guanine nucleotide binding to G proteins. J Biol Chem 1986;261:7393–7399. [PubMed: 3086311]

Fields TA, Casey PJ. Signalling functions and biochemical properties of pertussis toxin-resistant G-proteins. Biochem J 1997;321:561–571. [PubMed: 9032437]

Gilchrist A, Mazzoni MR, Dineen B, Dice A, Linden J, Proctor WR, Lupica CR, Dunwiddie TV, Hamm HE. Antagonists of the receptor-G protein interface block Gi-coupled signal transduction. J Biol Chem 1998;273:14912–14919. [PubMed: 9614095]

Hamm HE. How activated receptors couple to G proteins. Proc Natl Acad Sci U S A 2001;98:4819–4821. [PubMed: 11320227]

Hessling J, Lohse MJ, Klotz KN. Peptide G protein agonists from a phage display library. Biochem Pharmacol 2003;65:961–967. [PubMed: 12623127]

Higashijima T, Burnier J, Ross EM. Regulation of Gi and Go by mastoparan, related amphiphilic peptides, and hydrophobic amines. Mechanism and structural determinants of activity. J Biol Chem 1990;265:14176–14186. [PubMed: 2117607]

Higashijima T, Ferguson KM, Sternweis PC, Smigel MD, Gilman AG. Effects of Mg2+ and the beta gamma-subunit complex on the interactions of guanine nucleotides with G proteins. J Biol Chem 1987;262:762–766. [PubMed: 3100519]

Hooks SB, Waldo GL, Corbitt J, Bodor ET, Krumins AM, Harden TK. RGS6, RGS7, RGS9, and RGS11 stimulate GTPase activity of Gi family G-proteins with differential selectivity and maximal activity. J Biol Chem 2003;278:10087–10093. [PubMed: 12531899]

Hyde-DeRuyscher R, Paige LA, Christensen DJ, Hyde-DeRuyscher N, Lim A, Fredericks ZL, Kranz J, Gallant P, Zhang J, Rocklage SM, et al. Detection of small-molecule enzyme inhibitors with peptides isolated from phage-displayed combinatorial peptide libraries. Chem Biol 2000;7:17–25. [PubMed: 10662687]

Iiri T, Farfel Z, Bourne HR. G-protein diseases furnish a model for the turn-on switch. Nature 1998;394:35–38. [PubMed: 9665125]

Ja WW, Roberts RW. In vitro selection of state-specific peptide modulators of G protein signaling using mRNA display. Biochemistry 2004;43:9265–9275. [PubMed: 15248784]

Jones TA, Zou JY, Cowan SW, Kjeldgaard. Improved methods for building protein models in electron density maps and the location of errors in these models. Acta Crystallogr A 1991;47:110–119. [PubMed: 2025413]

Kimple RJ, Kimple ME, Betts L, Sondek J, Siderovski DP. Structural determinants for GoLoco-induced inhibition of nucleotide release by Galpha subunits. Nature 2002;416:878–881. [PubMed: 11976690]

Kimple RJ, Willard FS, Hains MD, Jones MB, Nweke GK, Siderovski DP. Guanine nucleotide dissociation inhibitor activity of the triple GoLoco motif protein G18: alanine-to-aspartate mutation restores function to an inactive second GoLoco motif. Biochem J 2004;378:801–808. [PubMed: 14656218]

Lambright DG, Sondek J, Bohm A, Skiba NP, Hamm HE, Sigler PB. The 2.0 A crystal structure of a heterotrimeric G protein. Nature 1996;379:311–319. [PubMed: 8552184]

Marin EP, Krishna AG, Sakmar TP. Disruption of the alpha5 helix of transducin impairs rhodopsin-catalyzed nucleotide exchange. Biochemistry 2002;41:6988–6994. [PubMed: 12033931]

Martin EL, Rens-Domiano S, Schatz PJ, Hamm HE. Potent peptide analogues of a G protein receptor-binding region obtained with a combinatorial library. J Biol Chem 1996;271:361–366. [PubMed: 8550587]

McCudden CR, Hains MD, Kimple RJ, Siderovski DP, Willard FS. G-protein signaling: back to the future. Cell Mol Life Sci 2005;62:551–577. [PubMed: 15747061]

Mixon MB, Lee E, Coleman DE, Berghuis AM, Gilman AG, Sprang SR. Tertiary and quaternary structural changes in Gi alpha 1 induced by GTP hydrolysis. Science 1995;270:954–960. [PubMed: 7481799]

Navaza J. AMoRe: an automated package for molecular replacement. Acta Crystallogr A 1994;50:157–163.

Neubig RR, Siderovski DP. Regulators of G-protein signalling as new central nervous system drug targets. Nat Rev Drug Discov 2002;1:187–197. [PubMed: 12120503]

Palczewski K, Kumasaka T, Hori T, Behnke CA, Motoshima H, Fox BA, Le Trong I, Teller DC, Okada T, Stenkamp RE, et al. Crystal structure of rhodopsin: A G protein-coupled receptor. Science 2000;289:739–745. [PubMed: 10926528]

Remmers AE, Engel C, Liu M, Neubig RR. Interdomain interactions regulate GDP release from heterotrimeric G proteins. Biochemistry 1999;38:13795–13800. [PubMed: 10529224]

Rodi DJ, Makowski L, Kay BK. One from column A and two from column B: the benefits of phage display in molecular-recognition studies. Curr Opin Chem Biol 2002;6:92–96. [PubMed: 11827830]

Rondard P, Iiri T, Srinivasan S, Meng E, Fujita T, Bourne HR. Mutant G protein alpha subunit activated by Gbeta gamma: a model for receptor activation? Proc Natl Acad Sci U S A 2001;98:6150–6155. [PubMed: 11344266]

Ross EM. Quantitative assays for GTPase-activating proteins. Methods Enzymol 2002;344:601–617. [PubMed: 11771414]

Rossman KL, Der CJ, Sondek J. GEF means go: turning on RHO GTPases with guanine nucleotide-exchange factors. Nat Rev Mol Cell Biol 2005;6:167–180. [PubMed: 15688002]

Scott JK, Huang SF, Gangadhar BP, Samoriski GM, Clapp P, Gross RA, Taussig R, Smrcka AV. Evidence that a protein-protein interaction ′hot spot′ on heterotrimeric G protein betagamma subunits is used for recognition of a subclass of effectors. Embo J 2001;20:767–776. [PubMed: 11179221]

Slep KC, Kercher MA, He W, Cowan CW, Wensel TG, Sigler PB. Structural determinants for regulation of phosphodiesterase by a G protein at 2.0 A. Nature 2001;409:1071–1077. [PubMed: 11234020]

Snow BE, Brothers GM, Siderovski DP. Molecular cloning of regulators of G-protein signaling family members and characterization of binding specificity of RGS12 PDZ domain. Methods Enzymol 2002;344:740–761. [PubMed: 11771424]

Sparks, AB.; Adey, NB.; Cwirla, S.; Kay, BK. In Phage Display of Peptides and Proteins, A Laboratory Manual. In: Kay, BK.; Winter, J.; McCafferty, J., editors. Screening phage-displayed random peptide libraries. Academic Press; San Diego: 1996. p. 227-253.

Sprang SR. G protein mechanisms: insights from structural analysis. Annu Rev Biochem 1997;66:639–678. [PubMed: 9242920]

Sukumar M, Higashijima T. G protein-bound conformation of mastoparan-X, a receptor-mimetic peptide. J Biol Chem 1992;267:21421–21424. [PubMed: 1400455]

Sunahara RK, Tesmer JJ, Gilman AG, Sprang SR. Crystal structure of the adenylyl cyclase activator Gsalpha. Science 1997;278:1943–1947. [PubMed: 9395396]

Tall GG, Gilman AG. Purification and Functional Analysis of Ric-8A: A Guanine Nucleotide Exchange Factor for G-protein a Subunits. Methods Enzymol 2004;390:377–388. [PubMed: 15488189]

Tall GG, Krumins AM, Gilman AG. Mammalian Ric-8A (synembryn) is a heterotrimeric Galpha protein guanine nucleotide exchange factor. J Biol Chem 2003;278:8356–8362. [PubMed: 12509430]

Tesmer JJ, Berman DM, Gilman AG, Sprang SR. Structure of RGS4 bound to AlF4--activated G(i alpha1): stabilization of the transition state for GTP hydrolysis. Cell 1997a;89:251–261. [PubMed: 9108480]

Tesmer JJ, Sunahara RK, Gilman AG, Sprang SR. Crystal structure of the catalytic domains of adenylyl cyclase in a complex with Gsalpha.GTPgammaS. Science 1997b;278:1907–1916. [PubMed: 9417641]

Ulfers AL, McMurry JL, Miller A, Wang L, Kendall DA, Mierke DF. Cannabinoid receptor-G protein interactions: G(alphai1)-bound structures of IC3 and a mutant with altered G protein specificity. Protein Sci 2002;11:2526–2531. [PubMed: 12237474]

Wall MA, Coleman DE, Lee E, Iniguez-Lluhi JA, Posner BA, Gilman AG, Sprang SR. The structure of the G protein heterotrimer Gi alpha 1 beta 1 gamma 2. Cell 1995;83:1047–1058. [PubMed: 8521505]

Wall MA, Posner BA, Sprang SR. Structural basis of activity and subunit recognition in G protein heterotrimers. Structure 1998;6:1169–1183. [PubMed: 9753695]

Willard FS, Kimple RJ, Kimple AJ, Johnston CA, Siderovski DP. Fluorescence-based assays for RGS box function. Methods Enzymol 2004;389:56–71. [PubMed: 15313559]

Worthylake DK, Rossman KL, Sondek J. Crystal structure of Rac1 in complex with the guanine nucleotide exchange region of Tiam1. Nature 2000;408:682–688. [PubMed: 11130063]

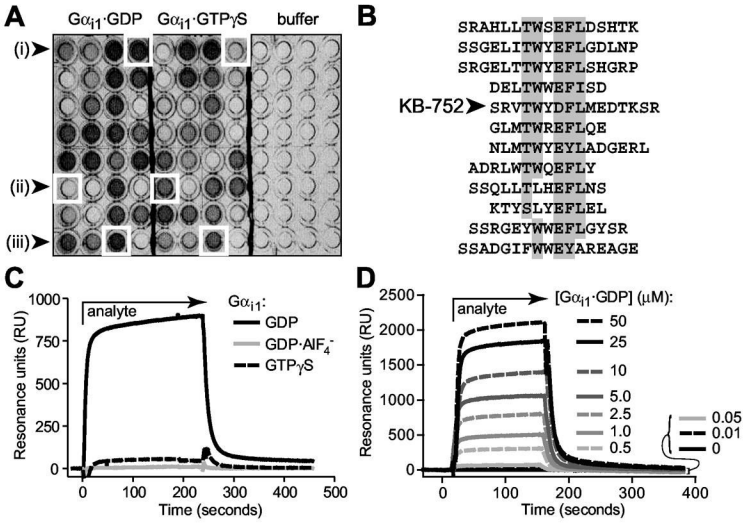

Figure 1.

Identification of nucleotide-dependent $G\alpha_i$-binding peptides via phage display. (**A**) Representative phage ELISA results indicating the identification of (i) GDP-selective, (ii) GTPγS-selective, and (iii) nucleotide state-independent $G\alpha_{i1}$-binding peptides. (**B**) Sequences of 12 isolated peptides with GDP-selective binding to $G\alpha_{i1}$, sharing a consensus $TWX^{E}/_{D}FL$ motif with the particular peptide used in this study: KB-752. (**C**) Nucleotide-dependent binding of KB-752 as measured by surface plasmon resonance (SPR). 5 μM $G\alpha_{i1}$ protein ("analyte"), in each of three nucleotide bound states, was injected over immobilized, biotinylated KB-752. Non-specific binding to a control peptide was subtracted from each curve. (**D**) GDP-bound $G\alpha_{i1}$ was injected at each indicated concentration over immobilized KB-752 to determine the dissociation constant (K_d) for this interaction pair. SPR-derived dissociation constants for the interaction of KB-752 with $G\alpha_{i1}$ and $G\alpha_o$, in their ground state (GDP-bound), transition state-mimetic (GDP·AlF_4^- bound), and activated state (GTPγS-bound) forms, were obtained from analyses (n = 4-6 for each state) similar to that shown in panel **D.** Dissociation constants of >1000 μM were obtained for both Gα subunits in their GDP·AlF_4^--bound form, and for $G\alpha_o$ bound to GTPγS.

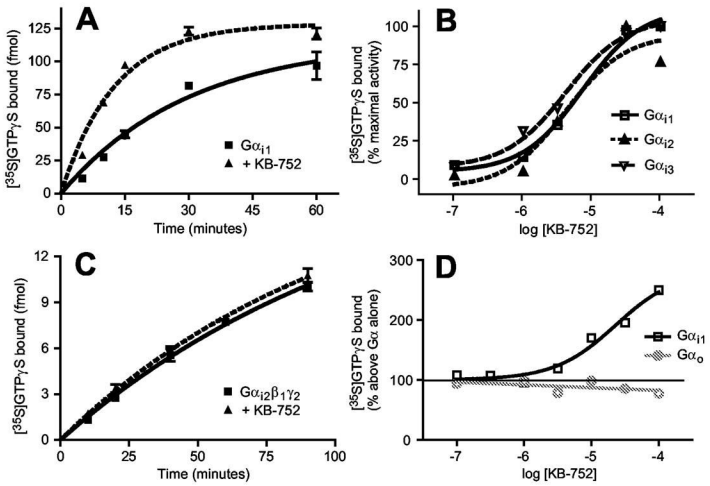

Figure 2.

KB-752 is a selective guanine nucleotide exchange factor for $G\alpha_i$ subunits. (**A**) KB-752 (10 μM) enhances the GTPγS binding rate of $G\alpha_{i1}$·GDP (50 nM); rate constants at 30 °C: $G\alpha_{i1}$ alone = 0.029 ± 0.006 min^{-1}, $G\alpha_{i1}$ + KB-752 = 0.086 ± 0.008 min^{-1}. (**B**) KB-752 is equipotent as a GEF on all three $G\alpha_i$ members. 50 nM $G\alpha_{i1}$, $G\alpha_{i2}$, or $G\alpha_{i3}$ was incubated with indicated concentrations of KB-752 and the amount of [^{35}S]GTPγS binding was measured after 10 min at 30°C, expressed as percent of maximal GTPγS binding. KB-752 does not alter the rate of GTPγS binding by (**C**) $G\alpha_i$-heterotrimer $G\alpha_{i2}$·GDP/$G\beta_1\gamma_2$ (peptide and protein amounts as in panel A), nor (**D**) isolated $G\alpha_o$·GDP. For the dose-response curve of panel (**D**), 50 nM $G\alpha_{i1}$ or $G\alpha_o$ was incubated in the presence of the indicated concentrations of KB-752 and the amount of [^{35}S]GTPγS binding was measured (after 10 min at 30 °C for $G\alpha_{i1}$; after 5 min at 20 °C for $G\alpha_o$) as described in Experimental Procedures and is expressed as the percent of GTPγS bound in the absence of KB-752. The EC_{50} value for GEF activity on $G\alpha_{i1}$ was 5.6 ± 1.1 μM. Data shown are from a representative experiment of 3-5 independent experiments.

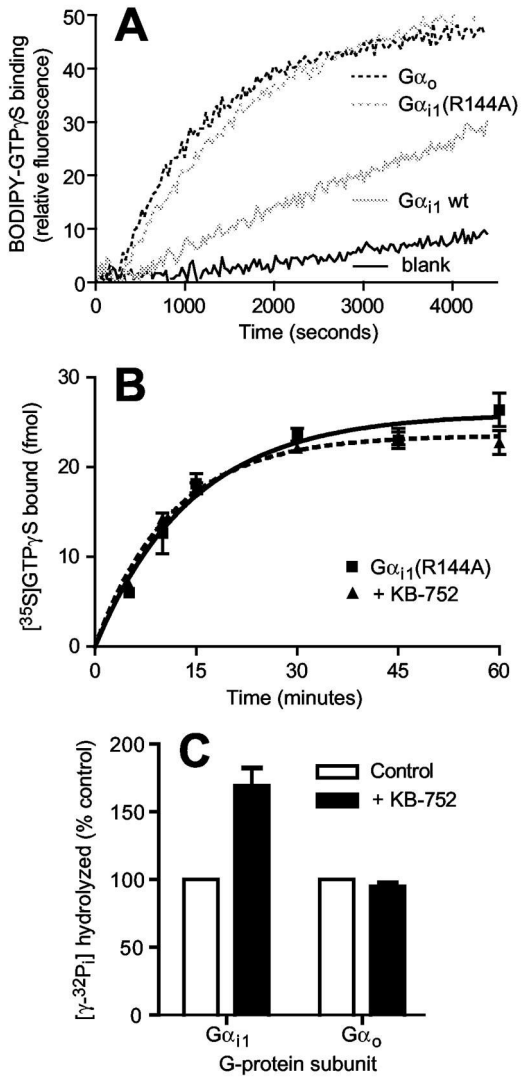

Figure 3.

KB-752 GEF activity increases steady-state GTP hydrolysis by $G\alpha_{i1}$, but does not act on a $G\alpha_{i1}$ point mutant (R144A) with accelerated spontaneous nucleotide release. (**A**) 200 nM of wild-type (wt) $G\alpha_{i1}$, R144A $G\alpha_{i1}$, or wild-type $G\alpha_o$ was added to cuvettes containing 1 μM BODIPY-FL-GTPγS. Real-time nucleotide binding (Kimple et al., 2004) was measured at 25 °C as an increase in fluorescence response (λ_{ex} = 485 nm; λ_{em} = 530 nm; slit widths of 3.0 nm) upon binding BODIPY-FL-GTPγS. Mutation of arginine 144 to alanine (R144A) resulted in $G\alpha_{i1}$ nucleotide binding kinetics indistinguishable from that of $G\alpha_o$, as previously reported by Remmers and colleagues (Remmers et al., 1999). (**B**) KB-752 does not alter the rate of GTPγS binding by the mutant $G\alpha_{i1}$ subunit (R144A) with accelerated spontaneous nucleotide exchange comparable to that of wildtype $G\alpha_o$ (experiment performed as in Figure 2A except conducted at 20 °C). (**C**) Confirming the GEF activity of KB-752 on wild type $G\alpha_{i1}$, addition of KB-752 (100 μM) to Gα (200 nM) enhances the steady-state hydrolysis of [γ^{32}-P]GTP by $G\alpha_{i1}$, but has no effect on $G\alpha_o$. Note that the rate-limiting step in steady-state hydrolysis of GTP by Gα subunits is release of product (*i.e.*, GDP) and not the hydrolysis of GTP *per se* (Ross, 2002).

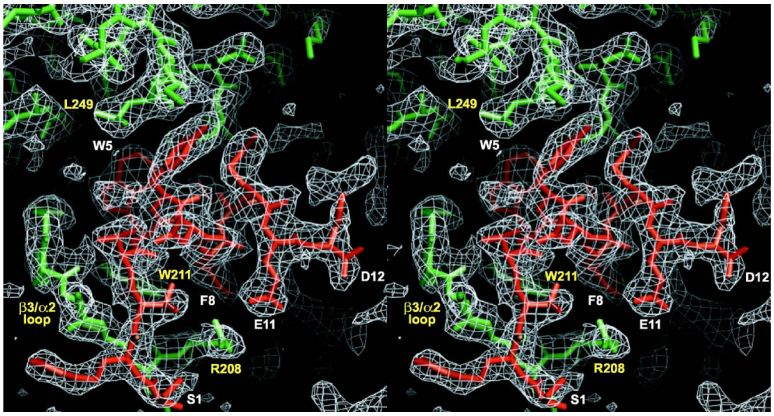

Figure 4.

Stereoview of experimental electron density for the KB-752 peptide bound to $G\alpha_{i1}$. The region highlighted is the entire peptide density (model in *red*; labels in *white*) found between switch II (α2 helix) and the α3 helix of $G\alpha_{i1}$ (model in *green*; labels in *yellow*). Shown is a $2F_o$-F_c simulated annealing composite omit map (generated with 5% overall model omitted) contoured at 1 s with electron density shown in white cage.

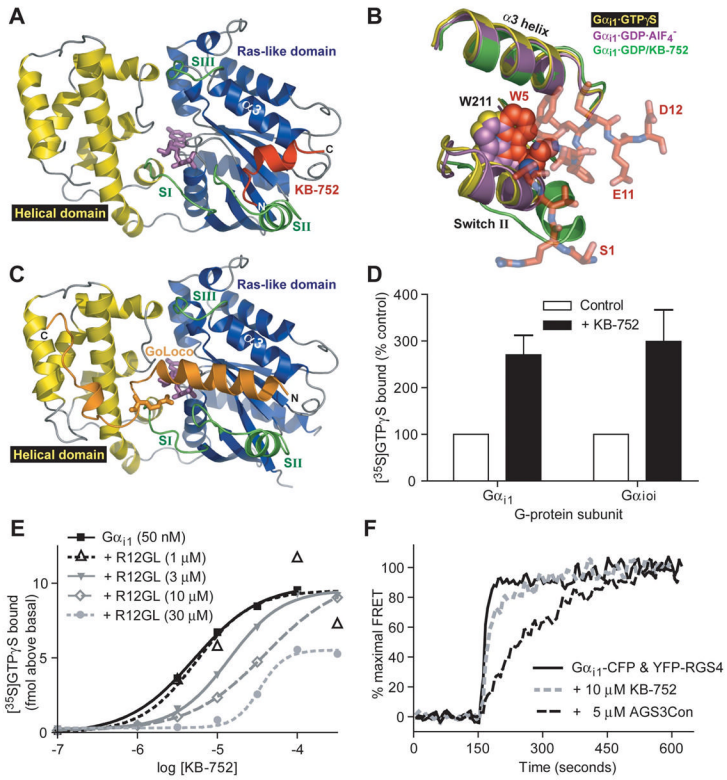

Figure 5.

Biochemical confirmation of the overall structural features of the $G\alpha_{i1}$/KB-752 interaction. (**A**) Ribbon trace of KB-752 (*red*) bound between the α2 ("switch II") and α3 helices of the $G\alpha_{i1}$ Ras-like domain (*blue*). No contacts are made between KB-752 and the all-helical domain (*yellow*) or bound GDP (*magenta*). Switch regions are denoted in *green*. (**B**) Structural basis for nucleotide selective binding of KB-752 to $G\alpha_{i1}$. KB-752 peptide (*red*, translucent) binds $G\alpha_{i1}$ between switch II and the α3 helix; the conformations of these two helices are shown for $G\alpha_{i1}$·GDP/KB-752 (*green*), $G\alpha_{i1}$·GTPγS (*yellow*), and $G\alpha_{i1}$·GDP·AlF_4^- (*magenta*). Whereas the α3 helix is not significantly altered, switch II is displaced to accommodate KB-752 binding. Switch II in both $G\alpha_{i1}$·GTPγS and $G\alpha_{i1}$·GDP·AlF_4^- assumes an extended α-helical conformation that is stabilized relative to $G\alpha_{i1}$·GDP (Mixon et al., 1995; Sprang, 1997). This conformation of switch II is not permissive to KB-752 binding as it creates extensive steric hindrance. In particular, W211 of switch II (shown in space filling) is in a restrictive position relative to W5 of KB-752. (**C**) The GoLoco motif of RGS14 (*orange*) is also seen to bind, in an alpha-helical conformation, between switch II and the α3 helix of $G\alpha_{i1}$ (PDB ID 1KJY); highlighted within the C α-carbon ribbon trace of the GoLoco peptide. Other features are colored as in panel A. (**D**) KB-752 GEF activity does not rely on the all-helical domain. 100 nM of $G\alpha_{i1}$ or a chimeric α containing the Ras-like domain of $G\alpha_{i1}$ and the all-helical domain of $G\alpha_o$ ("Gαioi"; ref. (Remmers et al., 1999) was incubated in the absence or presence of 50 μM KB-752 and [^{35}S]GTPγS binding after 10 min at 30 °C was measured as described in Experimental Procedures. Data are expressed as percent GTPγS bound relative to Gα protein in the absence of KB-752 ("Control") and are the average ± SEM of 4 independent experiments. (**E**) The KB-752 binding site on $G\alpha_{i1}$ overlaps that of GoLoco motif peptides. $G\alpha_{i1}$ (50 nM) was incubated in the absence or presence of the indicated concentrations of a peptide representing the GoLoco motif of RGS12 (R12GL) (Kimple et al., 2002). GTPγS binding was then measured in the presence of the indicated concentrations of KB-752. Data are expressed as fmol of GTPγS bound above that measured in the absence of KB-752 and are from a

representative experiment of 3 independent experiments. (**F**) The binding of KB-752 has no effect on the kinetics of $G\alpha_{i1}$ activation by AlF_4^-, unlike the slowed activation rate seen upon GoLoco peptide binding. $G\alpha_{i1}$-CFP (200 nM) and YFP-RGS4 (280 nM) fusion proteins, previously shown to generate increased fluorescence resonance energy transfer (FRET) upon $G\alpha_{i1}$ activation by AlF_4^- and subsequent RGS-box binding (Willard et al., 2004), were mixed together and pre-incubated with either 10 μM KB-752 peptide or 5 μM GoLoco consensus peptide (AGS3Con; Kimple et al., 2002), prior to the addition of NaF and AlCl 3 to final concentrations of 20 mM and 30 μM, respectively, at the 150-second mark.

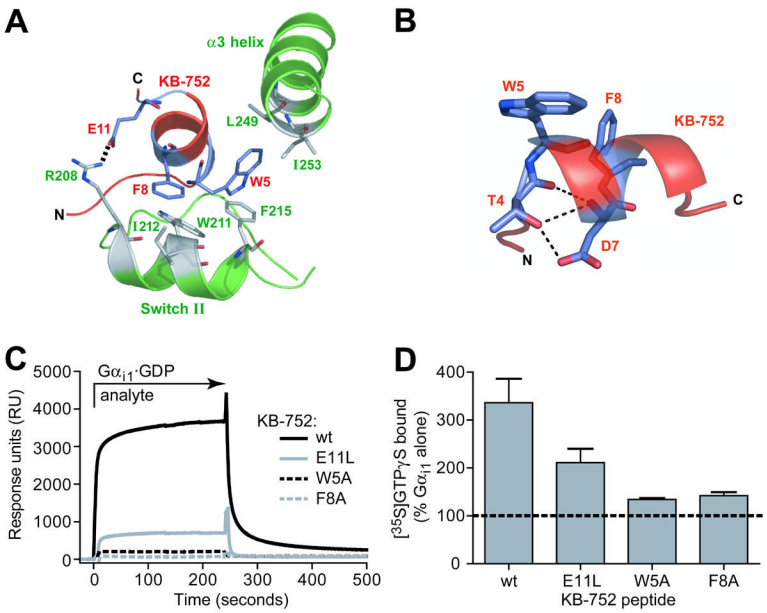

Figure 6.

Biochemical confirmation of specific interactions between KB-752 and $G\alpha_{i1}$. (**A**) Positions of KB-752 residues W5, F8, and E11 relative to residues in the switch II and α3 helices of $G\alpha_{i1}$. W5 and F8 are placed within hydrophobic pockets formed by $G\alpha_{i1}$ residues F215, L249, and I253, and W211, I212, and F215, respectively. E11 forms a salt bridge with R208 of $G\alpha_{i1}$. (**B**) Peptide residues T4 and D7 of the conserved $TWX^{E}/_{D}FL$ binding motif form an intrapeptide hydrogen bond network that helps to orient W5 and F8. (**C, D**) Effects of W5A, F8A, and E11L mutations to KB-752 activity. (**C**) Indicated KB-752 mutant or wildtype (wt) peptides were each immobilized to a density of ~1000 RUs on separate streptavidin-coated flow cells and 50 μM GDP-bound $G\alpha_{i1}$ ("analyte") was injected simultaneously over all four surfaces. (**D**) Compared to the increase in GTPγS binding observed by addition of 50 μM wildtype KB-752 to 100 nM $G\alpha_{i1}$·GDP, substantial reduction of GEF activity is seen upon mutation to the W5, F8, or E11 residue of KB-752.

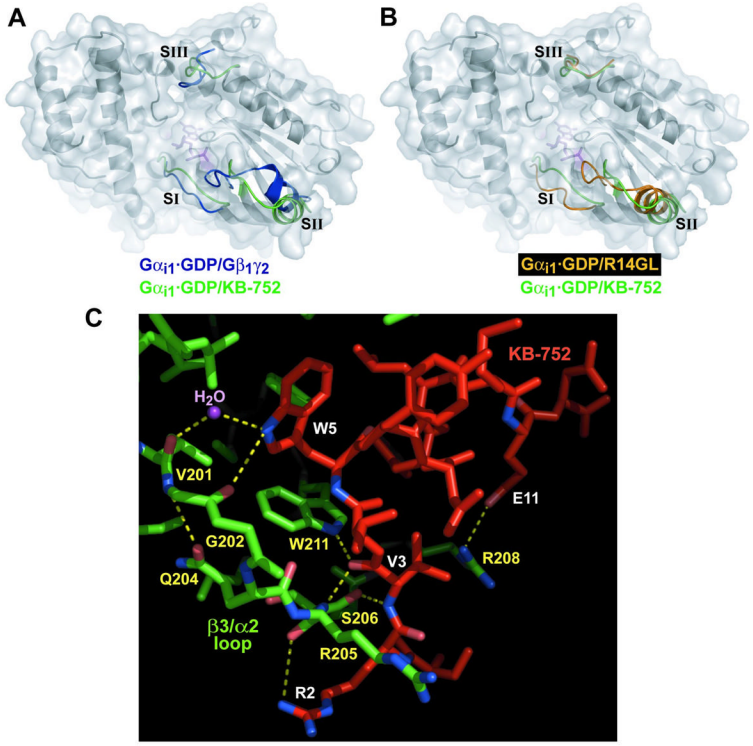

Figure 7.

Conformational changes in Gα switch regions induced by KB-752 binding. (**A,B**) Relative orientations of the three switch regions (SI — III) in heterotrimeric (PDB code 1GP2; *blue* in panel **A**), $G\alpha_{i1}$·GDP/R14GL (PDB code 1KJY; *orange* in panel **B**), and $G\alpha_{i1}$·GDP/KB-752 (*green*). Movement of switch II (α2 helix) and the connected β3/α2 loop away from the nucleotide binding pocket in $G\alpha_{i1}$·GDP/KB-752 is thought to contribute to GEF activity by creating a route for GDP release. The RGS14 GoLoco motif peptide (R14GL) displaces switch II but does not significantly alter the position of the β3/α2 loop. (**C**) Binding of KB-752 displaces switch II resulting in a reorientation of the β3/α2 loop away from the guanine nucleotide pocket. KB-752 (*red*) stabilizes the β3/α2 loop (*green*) via several hydrogen bonds (indicated as *yellow* dashes), including the carbonyl oxygen of G202 (Gα) with the indole nitrogen of W5 (KB-752), and the side chain hydroxyl and main chain amide nitrogen of S206 (Gα) with the main chain amide nitrogen and carbonyl oxygen of V3 (KB-752), respectively. A water molecule (*magenta* ball) is coordinated by both Gα and KB-752 contacts.

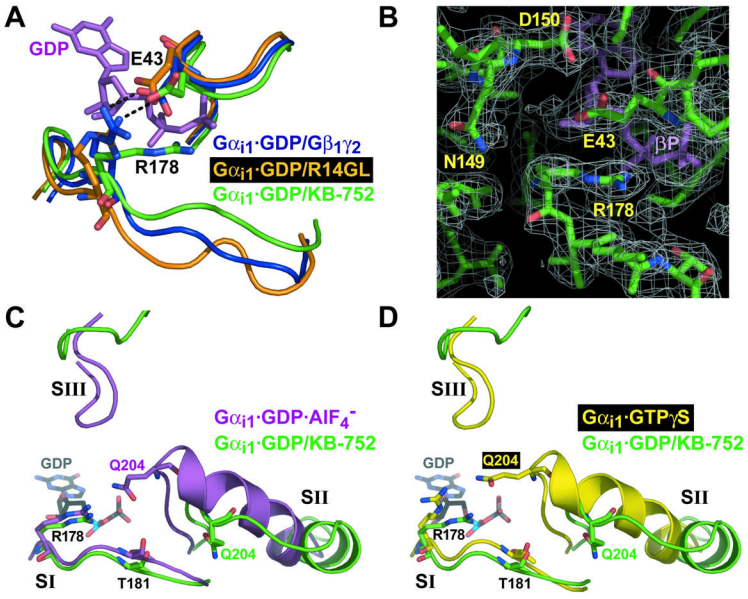

Figure 8.

Comparison of switch regions and core catalytic residues of KB-752-bound $G\alpha_{i1}$ with other states of $G\alpha_{i1}$. (**A**) Movement of switch I in the $G\alpha_{i1}$·GDP/KB-752 complex (*green*), versus its position in the $G\alpha_{i1}\beta_1\gamma_2$ heterotrimer (*blue*) and the $G\alpha_{i1}$·GDP/R14GL complex (*orange*), results in disruption of a salt-bridge (*black* dotted line) between R178 and E43 that normally stabilizes bound GDP (*magenta*) within $G\alpha_{i1}$ when complexed to a GDI (Gβγ or GoLoco peptide). (**B**) Electron density of the R178 side-chain in the $G\alpha_{i1}$·GDP/KB-752 complex (from a 2Fo-Fc simulated annealing composite omit map contoured to a level of 1 σ) is denoted by white mesh. In the background is the beta-phosphate of the bound GDP (βP). (**C,D**) Switch region comparisons with activated $G\alpha_{i1}$ states. Switch regions of $G\alpha_{i1}$·GDP/KB-752 (*green*), $G\alpha_{i1}$·GDP·AlF_4^- (PDB code 1GFI; *magenta*; panel **C**), and $G\alpha_{i1}$·GTPγS (PDB code 1GIA; *yellow*; panel **D**), are shown along with the residues critical for GTP hydrolysis (R178 and T181 within switch I and Q204 within switch II). GDP from the $G\alpha_{i1}$·GDP/KB-752 structure is shown for reference in each case. Overall conformation of the switch regions of $G\alpha_{i1}$·GDP·AlF_4^- and $G\alpha_{i1}$·GTPγS are very similar, save for key changes in the position of catalytic residue side chains (Wall et al., 1998). Whereas switch I of $G\alpha_{i1}$·GDP/KB-752 is very similar to that of the activated forms, both switch II and III are dramatically removed from the guanine nucleotide to allow for GDP release. The catalytic Q204 residue within switch II is far removed from the bound nucleotide and active site for GTP hydrolysis in the $G\alpha_{i1}$·GDP/KB-752 structure. However, R178 and T181 of switch I are in a strikingly similar position to that of the $G\alpha_{i1}$·GDP·AlF_4^- structure.

Table 1

Data collection and refinement statistics

Data collection[a]	
Space group	$P2_1$
No. of molecules per asymmetric unit	4
Unit cell dimensions	
a, b, c (Å)	72.9, 112.8, 109.5
α, β, γ (°)	90, 93.8, 90
Wavelength (Å)	1.0093
Resolution (Å)	50-2.5 (2.59-2.5)
R_{symm} (%)	26.6
Linear R-factor[b]	0.072 (0.266)
Square R-factor[c]	0.065 (0.232)
$<I\sigma I>$[d]	24 (3.6)
Completeness (%)	96.4 (89.6)
Redundancy	3.5
Refinement	
Resolution (Å)	20-2.5 (2.53-2.5)
No. reflections (working/test)	29795/1561
R_{work}/R_{free} (%)[e]	24.9/28.1
No. of nonhydrogen protein atoms	10584
GDP molecules	4
Water molecules	136
R.m.s. deviations	
Bonds (Å)	0.062
Angles (°)	1.9
Overall B-factors (chain B:chain F dimer)	
G-alpha	41.9 (38.2)
KB-752 peptide	52.4 (43.9)
GDP	35.6 (32.6)
Water	32.5
Ramachandran plot (% in region)	
Most favored	88.6
Allowed	9.0
Generously allowed	2.4
Disallowed	0.0

[a] Numbers in parentheses pertain to the highest resolution shell.

[b] Linear R-factor = $\Sigma(|I - <I>|)/\Sigma(I)$

[c] Square R-factor = $\Sigma(|I - <I>|)^2 /\Sigma(I)^2$

[d] $<I/\sigma I>$, Mean signal-to-noise, where I is the integrated intensity of a measured reflection and σI is the estimated error in measurement.

[e] $R_{work} = \Sigma(|F_p - F_{p(calc)}|)/\Sigma F_p$, where F_p and $F_{p(calc)}$ are the observed and calculated structure factor amplitudes. R_{free} is calculated similarly using test set reflections never used during refinement.